Int. J. Heat Mass Transfer. Vol. 30, No. 4, pp. 717–727, 1987
Printed in Great Britain

0017–9310/87 $3.00 + 0.00

The Brinkman model for boundary layer regime in a rectangular cavity with uniform heat flux from the side

P. VASSEUR and L. ROBILLARD

Ecole Polytechnique, Campus de l'Universite de Montreal, Case postale 6079, succursale A, Montreal, P.Q., Canada H3C 3A7

(*Received* 1 *May* 1986 *and in final form* 4 *August* 1986)

Abstract—This paper summarizes an analytical and numerical study of natural convection in a rectangular porous layer subjected to uniform heat fluxes along its vertical boundaries. In the formulation of the problem, use is made of the Brinkman-extended Darcy model which allows the no-slip boundary condition to be satisfied. The boundary layer equations are solved using a modified Oseen linearization method. It is found that the boundary effects have a non-negligible influence on the flow field and heat transfer. These effects are more pronounced in high porosity media where the flow rate and heat transfer are significantly reduced. For low porosity media the results obtained on the basis of a pure Darcy's law model are recovered as a limiting case of the present theory. Numerical results are reported in the range $20 \leq R \leq 1000$, $10^{-7} \leq Da \leq 10$ and $2 \leq A \leq 4$. The boundary layer analytical solution is shown to agree well with the numerical results.

INTRODUCTION

NATURAL convection in saturated porous media has recently received considerable attention because of numerous applications in geophysics and energy related engineering problems. Such applications include geothermal reservoirs, porous insulations, packed-bed catalytic reactors, heat storage beds, nuclear waste disposal systems, sensible heat storage beds, and enhanced recovery of petroleum resources. Most analytical studies for natural convection in porous media are based on the Darcy flow model. One of the main advantages of Darcy's law is that it linearizes the momentum equation, thus removing a considerable amount of difficulty in solving the governing equations. On the other hand, since Darcy's law is of order one less than the Navier–Stokes it cannot account for the no-slip boundary condition on rigid boundaries. In order to take into consideration the boundary effect, which may become important in porous media with high porosities such as foam metals and fibrous media, Brinkman's extension of Darcy's law should be used.

By using Brinkman's equation Chan *et al.* [1] have considered numerically the problem of natural convection in an enclosed porous medium bounded by plane rectangular surfaces at different temperatures. It was found that when the Darcy number Da, based on the width of the enclosure, was less than 10^{-3} the results were in agreement with Darcy's law. A similar criterion has been reported by Cheng [2] while discussing the motion of a fluid in a horizontal layer of saturated porous medium uniformly heated from below. The Brinkman model was also used by Katto and Masuaka [3] as well as by Walker and Homsy [4] for the studies of onset of free convection of liquids in a porous medium bounded between parallel plates and heated from below. More recently, a boundary layer analysis for natural convection in a vertical porous enclosure has been performed by Tong and Subramanian [5]. The boundary layer equations, derived from the Brinkman model, were solved using the modified Oseen method. The flow field was found to be characterized by a parameter E defined as $R\,Da/A$ where both the Rayleigh number R and Darcy number Da are based on the width of the cavity and A is the cavity aspect ratio. It was observed that the Darcy results agreed with their solution to within 1% when $E <$ order 10^{-4}. However, for higher values of E the heat transfer was found to be significantly below the value predicted by Darcy's law. Furthermore, by comparing the experimental data reported by Klarsfeld [6] with the theoretical results predicted both by Darcy's and Brinkman's equations it was concluded by Tong and Subramanian that the Brinkman model offered the best agreement with the experimental results. The fact that, for high porosity media, Darcy's model may incorrectly overpredict the heat transfer has also been observed for the case of natural convection from a vertical plate embedded in a porous medium. From Brinkman's equation and the boundary layer approximation Evans and Plumb [7] have demonstrated that the boundary effect can be neglected only when the Darcy number, based on the length of the plate, was less than 10^{-7}. Other studies [8–10], using both numerical and perturbation methods, have shown that in fact the boundary effect depended on the ratio of the momentum and thermal boundary layer thicknesses. For low porosity media the thickness of the viscous layer, which is caused by

NOMENCLATURE

A	aspect ratio, H'/L'
C_p	specific heat at constant pressure
Da	Darcy number, K/L'^2
g	gravitational acceleration
H'	vertical dimension
k	thermal conductivity of fluid-saturated porous medium
K	permeability
L'	horizontal dimension
Nu	Nusselt number, equation (26)
p'	pressure
$p(y)$	even function, equation (17)
Q	vertical flow rate, equation (41)
q'	constant heat flux
$q(y)$	odd function, equation (17)
R	Darcy–Rayleigh number, $g\beta KL'^2q'/k\alpha\nu$
Ra	Rayleigh number, R/Da
t	dimensionless time, $t'\alpha/L'^2$
T'	temperature
T'_0	reference temperature at the geometric center of the cavity
T'_∞	core temperature
ΔT	wall-to-wall temperature difference at $y = \text{const.}$
u	dimensionless horizontal velocity component, $u'L'/\alpha$
u_∞	dimensionless horizontal velocity in the core region, $u'_\infty L'/\alpha$
v	dimensionless vertical velocity component, $v'L'/\alpha$
x	dimensionless horizontal position, x'/L'
y	dimensionless position, y'/L'.

Greek symbols

α	effective thermal diffusivity
β	thermal expansion coefficient
μ	viscosity of the fluid
ν	kinematic viscosity of the fluid, μ/ρ
ρ	density
ψ	stream function, ψ'/α
ψ_∞	core stream function, ψ'_∞/α
ω	vorticity, $\omega'L'^2/\alpha$.

Superscript

$'$	dimensional quantities.

Subscript

∞	solution in the core region.

the no-slip boundary condition, becomes in general much smaller than the thermal boundary layer. As a result the no-slip condition can be neglected and Darcy's model is satisfactory. However, for high porosity media, the boundary effect can be quite important when the thickness of the viscous layer is more than or of the same order as that of the thermal boundary layer. For this situation Darcy's model will incorrectly overpredict the heat transfer [9] and flow rate [11].

The object of the present work is to study the boundary effect on the natural convection heat transfer in a rectangular medium heated and cooled with uniform heat flux along the vertical side walls. This problem has been considered in the past by Bejan [12] on the basis of the boundary layer and Darcy's approximations. The inertia effect on the heat transfer, which may become important when the Reynolds number based on the mean pore diameter is of order one or greater, has been discussed recently by Poulikakos [13]. In this study the boundary effect, though not important in low porosity media, is shown to be significant in high porosity media.

PROBLEM STATEMENT AND BOUNDARY LAYER ANALYSIS

Consider natural convection in an enclosed porous medium with rectangular, impermeable boundaries. The width and height of the model are L' and H', respectively (Fig. 1). The horizontal-end walls are insulated while the system is heated along the right-hand side and cooled along the left-hand side uniformly, i.e.

$$q' = k\left(\frac{\partial T'}{\partial x'}\right)_{x'=0,L'}. \tag{1}$$

Making the Boussinesq approximation and assuming constant properties, the governing equations with inertial and thermal dispersion effects neglected are

$$\nabla^2\psi' = \frac{K}{\mu}\left[\mu\nabla^4\psi' + \rho g\beta\frac{\partial T'}{\partial x'}\right] \tag{2}$$

$$\nabla^2 T' = \frac{\rho C_p}{k}\left[\frac{\partial\psi'}{\partial y'}\frac{\partial T'}{\partial x'} - \frac{\partial\psi'}{\partial x'}\frac{\partial T'}{\partial y'}\right] \tag{3}$$

$$u' = \frac{\partial\psi'}{\partial y'}, \qquad v' = -\frac{\partial\psi'}{\partial x'} \tag{4}$$

where ψ' is the usual stream function and u', v', T', K, g, β, ρ, and C_p represents the volume-averaged fluid velocity components, the local equilibrium temperature between the fluid and the porous solid, the permeability of the porous matrix, the gravitational acceleration, the coefficient of thermal expansion of the fluid, the effective thermal conductivity, the fluid density and the specific heat at constant pressure, respectively.

The above system is reduced to dimensionless form by introducing the following scales relating dimensional and non-dimensional quantities

$$x, y = (x', y')/L', \qquad u, v = (u', v')/(\alpha/L')$$
$$T = (T' - T_0')/\Delta T', \qquad \Delta T' = (q'L')/k \tag{5}$$
$$R = \frac{g\beta K L' \Delta T'}{\alpha \nu}, \qquad \psi = \psi'/\alpha$$

where T_0' is the temperature at the geometric center of the cavity; $\Delta T'$ a characteristic temperature difference and R is a Rayleigh number based on the constant heat flux q' and the permeability K of the medium.

The resulting non-dimensional system corresponding to equations (2)–(4) becomes

$$\nabla^2 \psi = Da \nabla^4 \psi - R \frac{\partial T}{\partial x} \tag{6}$$

$$\nabla^2 T = \frac{\partial \psi}{\partial y}\frac{\partial T}{\partial x} - \frac{\partial \psi}{\partial x}\frac{\partial T}{\partial y} \tag{7}$$

where $Da = K/L'^2$ is the Darcy number.

The boundary conditions for equations (6) and (7) are given by

$$\begin{aligned} &\text{at } x = 0, 1: && \psi = 0, && \frac{\partial \psi}{\partial x} = 0, && \frac{\partial T}{\partial x} = 1 \\ &\text{at } y = \pm \frac{A}{2}: && \psi = 0, && \frac{\partial \psi}{\partial y} = 0, && \frac{\partial T}{\partial y} = 0 \end{aligned} \tag{8}$$

where $A = H'/L'$ is the cavity aspect ratio.

Of particular interest is the case of convection at large Rayleigh numbers, driven by boundary layer flows, where most of the fluid motion is confined to a thin layer along each vertical wall. Making the usual boundary layer simplifications, the approximate forms of equations (6) and (7) valid in the boundary layer regime can be obtained as

$$\frac{\partial u}{\partial x} + \frac{\partial v}{\partial y} = 0 \tag{9}$$

$$\frac{\partial v}{\partial x} = Da \frac{\partial^3 v}{\partial x^3} + R \frac{\partial T}{\partial x} \tag{10}$$

$$\frac{\partial^2 T}{\partial x^2} = u \frac{\partial T}{\partial x} + v \frac{\partial T}{\partial y}. \tag{11}$$

The corresponding dimensionless boundary conditions for the left boundary layer are

$$\begin{aligned} &x = 0 && u = v = 0, && \frac{\partial T}{\partial x} = 1 \\ &x \to \infty && \begin{cases} u \to u_\infty(y) \\ T \to T_\infty(y) \\ v \to 0 \end{cases} \end{aligned} \tag{12}$$

where u_∞ and T_∞ are the flow and temperature in the core of the cavity, outside the boundary layer.

The above system of equations is similar to that solved by Tong and Subramanian [5] in their study of the boundary layer regime in a rectangular porous cavity with isothermal vertical walls. The procedure followed in ref. [5] is based on the technique laid out by Gill [14] who used the modified Oseen method to solve the boundary layer equations for Newtonian fluid convection in an enclosure. Omitting the algebra already discussed in refs. [5, 12, 14, 15] the solution for the velocity and temperature field, subjected to the present set of boundary conditions given by equations (9)–(12) is

$$v = \frac{R(e^{-\lambda_1 x} - e^{-\lambda_2 x})}{Da(\lambda_1^3 - \lambda_2^3) - (\lambda_1 - \lambda_2)} \tag{13}$$

$$T = -\frac{Da(\lambda_1^2 e^{-\lambda_1 x} - \lambda_2^2 e^{-\lambda_2 x})}{Da(\lambda_1^3 - \lambda_2^3) - (\lambda_1 - \lambda_2)} + \frac{v}{R} + T_\infty. \tag{14}$$

The temperature profile (14) satisfies the uniform heat flux condition at $x = 0$. The unknown functions λ_1 and λ_2 are complex numbers with positive real parts and are in general a function of y. The temperature distribution outside the boundary layer region T_∞ is also a function of y. Once T_∞, λ_1 and λ_2 are determined, v and T are completely specified by equations (13) and (14), respectively.

The unknown functions $\lambda_1(y)$, $\lambda_2(y)$ and $T_\infty(y)$ are determined, by integrating the conservation of mass with respect to x, leading to

$$\psi_\infty = -\int_0^\infty v \, dx = \frac{R(\lambda_1 - \lambda_2)}{[Da(\lambda_1^3 - \lambda_2^3) - (\lambda_1 - \lambda_2)]\lambda_1 \lambda_2} \tag{15}$$

where $\psi_\infty(y)$ is the dimensionless core stream function.

Similarly integration of the energy conservation equation and combination with equations (13) and (14) yields

$$\frac{d}{dy}\left[\frac{\psi_\infty^2}{2R^2}\frac{\lambda_1 \lambda_2}{\lambda_1 + \lambda_2}(Da\,\lambda_1 \lambda_2 + 1)\right] - \psi_\infty T_\infty' = -1. \tag{16}$$

Making use of the fact that the core flow must be centrosymmetric about $x = 1/2$ and $y = 0$ it is advantageous to express equations (15) and (16) in terms of Gill's functions [14]

$$\begin{aligned} p(y) &= \text{even function} \\ q(y) &= \text{odd function} \end{aligned} \tag{17}$$

where

$$\lambda_{1,2} = p\frac{(1-q)}{4}\left[1 \pm \sqrt{\left(\frac{8(1+q)}{Da\,p^2(1-q)^2} - (1+2q)\right)}\right]. \tag{18}$$

Substituting equation (18) into equations (15) and (16) and observing that ψ_∞, T_∞' and p are even functions, it is deduced that the odd function q must be zero and p and T_∞' must be constants. It follows from this

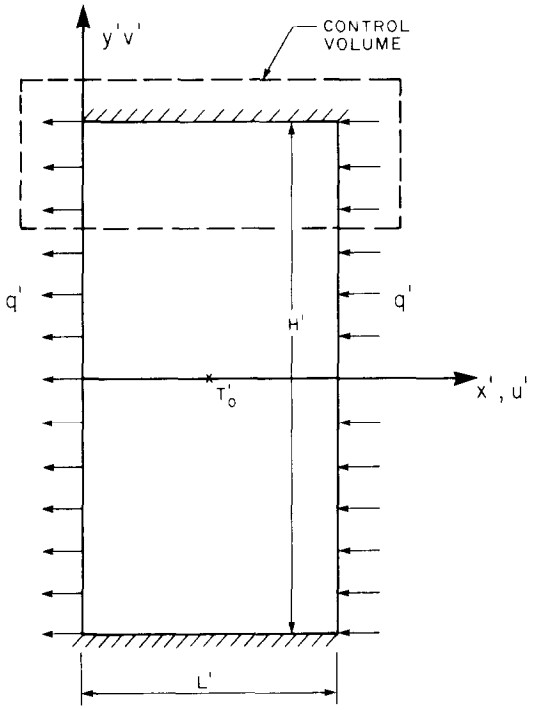

FIG. 1. Definition sketch.

result that the solution, for the present problem, is given by

$$\lambda_{1,2} = \frac{P}{4}\left(1 \pm \sqrt{}\right) \tag{19}$$

$$\psi_\infty = \frac{64DaR}{(Da\,p^2 - 4)^2}, \quad T_\infty = \frac{y}{\psi_\infty}, \quad u_\infty = 0 \tag{20}$$

$$v = -\frac{32}{\sqrt{}}\frac{R}{p(Da\,p^2 - 4)}\sinh\left(\frac{p}{4}\sqrt{}x\right)e^{-px/4} \tag{21}$$

$$T = \frac{-4Da\,p}{(Da\,p^2 - 4)}\cosh\left(\frac{p}{4}\sqrt{}x\right)e^{-px/4} + \frac{v}{2R} + T_\infty \tag{22}$$

where $\sqrt{} = \sqrt{(8/Da\,p^2 - 1)}$.

The value of the constant p is determined by considering the arbitrary control volume of Fig. 1. Integrating the equation of energy, equation (11), and making use of the thermal boundary conditions applied on the solid boundaries, namely constant heat flux on the vertical walls and zero heat flux through the horizontal wall, one obtains the following equation

$$\int_0^{L'} \rho C_p v' T' \,dx' = \int_0^{L'} k\frac{\partial T'}{\partial y'}\,dx' \tag{23}$$

at any position y'.

Writing expressions similar to equations (21) and (22) for the boundary layer flowing up along the right vertical wall and substituting these along with equations (21) and (22) into equation (23) yields upon integration and routine algebra

$$\frac{p(Da\,p^2 - 4)^5}{Da^2(Da\,p^2 + 4)} = 8192R^2. \tag{24}$$

The Nusselt number predicted by the present analysis is derived by first evaluating the wall-to-wall dimensionless temperature difference

$$\Delta T = T_{x=1} - T_{x=0} = \frac{8Da\,p}{(Da\,p^2 - 4)}. \tag{25}$$

It is noted that the temperature difference between the two vertical walls is independent of altitude y. The Nusselt number is thus given by

$$Nu = \left(\frac{q'}{\overline{\Delta T'}}\right)\frac{L'}{k} = \frac{1}{\Delta T} = \frac{(Da\,p^2 - 4)}{8Da\,p} \tag{26}$$

where $\overline{\Delta T'}$ is the actual wall-to-wall temperature difference.

It is well known that the Brinkman equation reduces to the Darcy equation as the permeability $K \to 0$ and to the Navier–Stokes equation as $K \to \infty$. Hence we can check the previous results for two special cases.

(1) $Da \ll 1$: *the Darcy medium situation*

Taking the limit of equation (24) for $Da \to 0$, it is found that $p \approx 2(Da^{-1/2} + R^{2/5})$. Substituting this result in equations (19)–(22) and (26) it may be shown that the flow field and temperature field reduce to

$$v = -R^{3/5}e^{-R^{2/5}x} \qquad \text{for } x \neq 0 \tag{27}$$

$$T = -R^{-2/5}e^{-R^{2/5}x} + T_\infty \tag{28}$$

$$\psi_\infty = R^{1/5}, \qquad T_\infty = \frac{y}{\psi_\infty} \tag{29}$$

$$Nu = \frac{1}{2}R^{2/5}. \tag{30}$$

The boundary layer regime in a Darcy porous layer with uniform heat flux from the side has been considered in the past by Bejan [12] for the case of a vertical layer and by Vasseur *et al.* [16] for the case of an inclined layer. The above equations, when translated into corresponding notations, are the same as those obtained in refs. [12, 16].

(2) $Da \gg 1$: *the viscous fluid situation*

Taking the limit of equation (24) for $Da \to \infty$ the value of p is obtained as $p \approx (8192Ra^2)^{1/9}$, where

$Ra = R\,Da^{-1}$. Substituting this result into equations (19)–(22) and (26) one obtains

$$v = -\frac{32}{p^3} Ra\, e^{-px/4} \sin\left(\frac{p}{4}x\right) \quad \text{for } \forall x \tag{31}$$

$$T = -\frac{4}{p} e^{-px/4} \cos\left(\frac{p}{4}x\right) + T_\infty \tag{32}$$

$$\psi_\infty = \frac{64}{p^4} Ra, \qquad T_\infty = \frac{y}{\psi_\infty} \tag{33}$$

$$Nu = \frac{p}{8} \tag{34}$$

which are similar to the results obtained in ref. [15] for the case of a rectangular cavity filled with a viscous fluid.

NUMERICAL SIMULATIONS

The vorticity–stream function formulation of the complete governing equations (6)–(8) is

$$\frac{\partial \omega}{\partial t} + \omega = Da \nabla^2 \omega + R \frac{\partial T}{\partial x} \tag{35}$$

$$\frac{\partial T}{\partial t} + \frac{\partial uT}{\partial x} + \frac{\partial vT}{\partial y} = \nabla^2 T \tag{36}$$

$$\nabla^2 \psi = -\omega \tag{37}$$

$$u = \frac{\partial \psi}{\partial y}, \qquad v = -\frac{\partial \psi}{\partial x}. \tag{38}$$

The initial and boundary conditions are given by

$$\begin{aligned} u = v = \psi = \omega = 0; \quad & T = 0 \quad \text{at } t = 0 \\ u = v = \psi = 0; \quad & \frac{\partial T}{\partial x} = 1 \quad \text{at } x = 0, 1 \\ u = v = \psi = 0; \quad & \frac{\partial T}{\partial y} = 0 \quad \text{at } y = \pm\frac{A}{2}. \end{aligned} \tag{39}$$

The governing equations (35)–(38) under boundary conditions (39) can be numerically solved by the finite difference method. The alternate direction implicit procedure (ADI) is adopted to obtain from equation (36) the temperature profiles by using a uniform grid. The computational method involved differs slightly from that described by Mallison and de Vahl Davis [17]. The first and second derivatives are approximated by central differences and the time derivatives by a first-order forward difference. The finite difference form of the energy equation is written in conservative form for the advective term in order to preserve the conservative property [18]. The values of the stream function at all grid points are obtained with equation (37) via a successive overrelaxation method (SOR). The stream function varying by less than 0.5×10^{-3} over all grid points was adopted as the convergence criterion. The velocities at all grid points are determined with equation (38) using updated values of the stream function.

In the present study, several different mesh sizes were used, the choice depending on the aspect ratio A of the cavity. The mesh size in the x-direction ranged from 30 to 50. In the x-direction a mesh size of $A/15$ to $A/25$ was chosen. A typical value of the time step was 0.005. The total time steps ranged from about 100 to 1000 and the corresponding computing time ranged from 60 to 300 s on the IBM 4381 computer.

To have an additional check on the accuracy of the results, an energy balance was used for the system. For this the heat transfer through each plane $x = \text{const.}$ was evaluated at each grid location $0 \le x \le 1$ and compared with the input at $x = 0$. For most of the results reported here the energy balance was satisfied to within 2% and never exceeded 5%.

RESULTS AND DISCUSSION

Based on the governing equations of motion and energy it is seen that the parameters affecting the convective heat transfer in the present problem are the Rayleigh number R, Darcy number Da and aspect ratio A. However, the theoretical results obtained both for a Darcian medium (equations (27)–(30)) and pure viscous fluid (equations (31)–(34)) show that the solution is independent of A. It has been demonstrated numerically in ref. [16] that this was indeed the case when A was approximately equal or greater than 2. The range of parameters considered in the present study are $20 \le R \le 1000$, $10^{-7} \le Da \le 10$ and $2 \le A \le 4$. In the following section the effects of different parameters are discussed.

Figure 2 illustrates typical streamlines and isotherm patterns for $R = 100$, $A = 2$ and $Da = 0$, 10^{-4}, 10^{-2} and 10^{-1}, respectively. For each map of Fig. 2 the increments between adjacent streamlines and isotherms are $\Delta\psi = \psi_{max}/8$ and $\Delta T = (T_{max} - T_{min})/10$, respectively, where ψ_{max} is the maximum value of the stream function and T_{max} and T_{min} the maximum and minimum values of the dimensionless temperature field located at the upper right-hand corner and lower left-hand corner of the cavity, respectively. Figure 2(a) illustrates the results obtained with Darcy's law, i.e. for $Da = 0$ and the fluid allowed to slip on the solid boundaries. This situation has been discussed in the past in refs. [12, 16]. The pattern of streamlines of Fig. 2(a) shows that a boundary layer of constant thickness develops near the vertical boundaries while the core fluid is stagnant. From the equal spacing of the isotherms a linear thermal vertical stratification both in the core and in the vertical boundary layers is deduced. In fact the temperature difference between vertical walls is independent of altitude since the wall temperatures increase linearly at the same rate as the vertical temperature gradient in the core region [12]. Finally

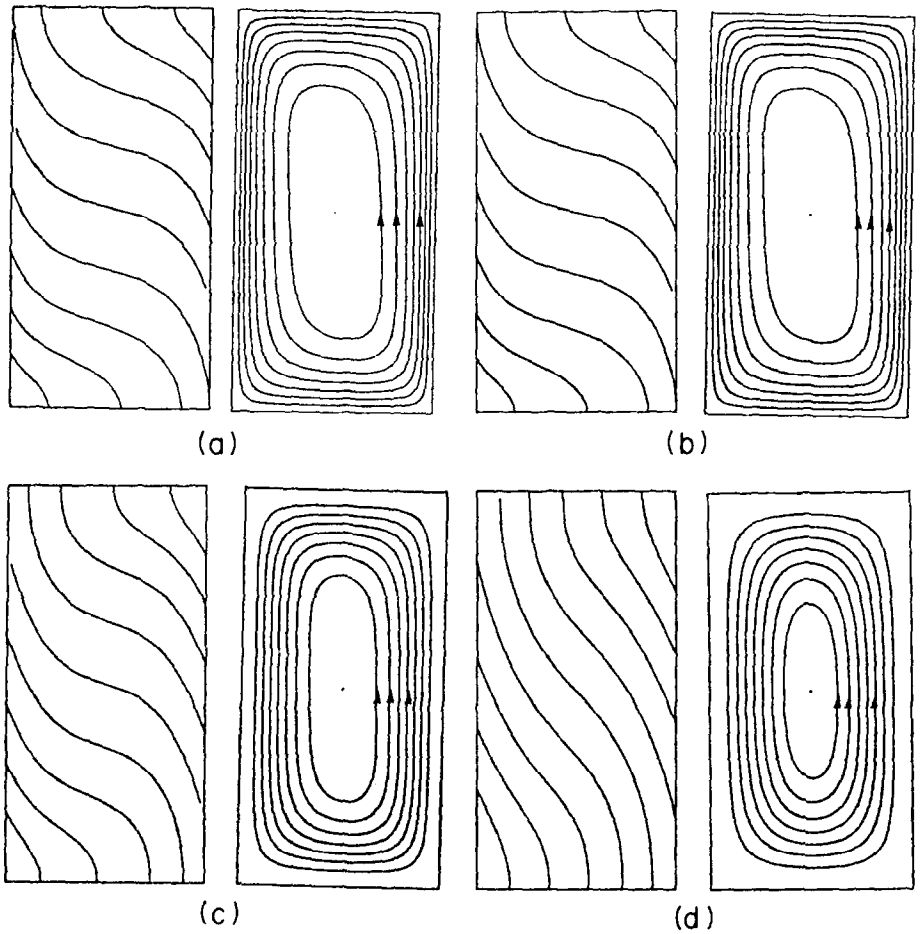

FIG. 2. Numerical solutions for the flow and temperature field $R = 100$, $A = 2$: (a) $Da = 0$, $\psi_{max} = 2.367$, $T_{max} = 0.644$, $T_{min} = -0.644$; (b) $Da = 10^{-4}$, $\psi_{max} = 2.352$, $T_{max} = 0.643$, $T_{min} = -0.633$; (c) $Da = 10^{-2}$, $\psi_{max} = 2.155$, $T_{max} = 6.703$, $T_{min} = -0.703$; (d) $Da = 10^{-1}$, $\psi_{max} = 1.291$, $T_{max} = 0.754$, $T_{min} = -0.754$.

the streamlines of Fig. 2(a) are observed to be closely spaced near the solid boundaries. This configuration indicates that the fluid velocity is a maximum on the boundaries as expected since Darcy's law allows the fluid to slip on them. Figures 2(b)–(d) illustrate typical results obtained on the basis of Brinkman's model for various values of Da. The results obtained with $Da = 10^{-4}$, Fig. 2(b), are seen to be qualitatively similar to those obtained by Darcy's law (Fig. 2(a)). This is expected since when Da is small enough, i.e. for low porosity media, the viscous term which is responsible for the boundary effects becomes negligible and Darcy's law correctly describes the flow behavior. However, as the porosity of the solid matrix (i.e. Da) is increased the influence of the boundary effects on the flow and temperature fields becomes significant. This is illustrated in Figs. 2(c) and (d) where the streamlines are observed to become relatively more and more sparsely spaced near the solid boundaries as the value of Da increases. This is due to the fact that the viscous term (Brinkman) becomes gradually more important and slows down the fluid in the neighborhood of the walls. It is also observed that the region where the flow has a maximum velocity, as indicated by closely spaced streamlines, moves away from the walls towards the core region as Da is increased. The sequence of Fig. 2 illustrates also the effects of Da on the isotherm field. When Da is small the convective motion inside the cavity is strong and the isotherms are considerably distorted. The flat isotherms in the core indicate a negligible lateral conduction. As Da is increased the viscous effects become more important and slow down the buoyancy-induced flow inside the cavity. The isotherm profiles become more linear and heat transfer across the cavity results from the combined action of conduction and convection.

Figure 3 shows the vertical velocity profiles at mid-height of the enclosure for $R = 300$ and various values of Da. Since the viscous forces are accounted for in Brinkman's model the no-slip boundary condition is satisfied and the velocity at the wall is zero. The

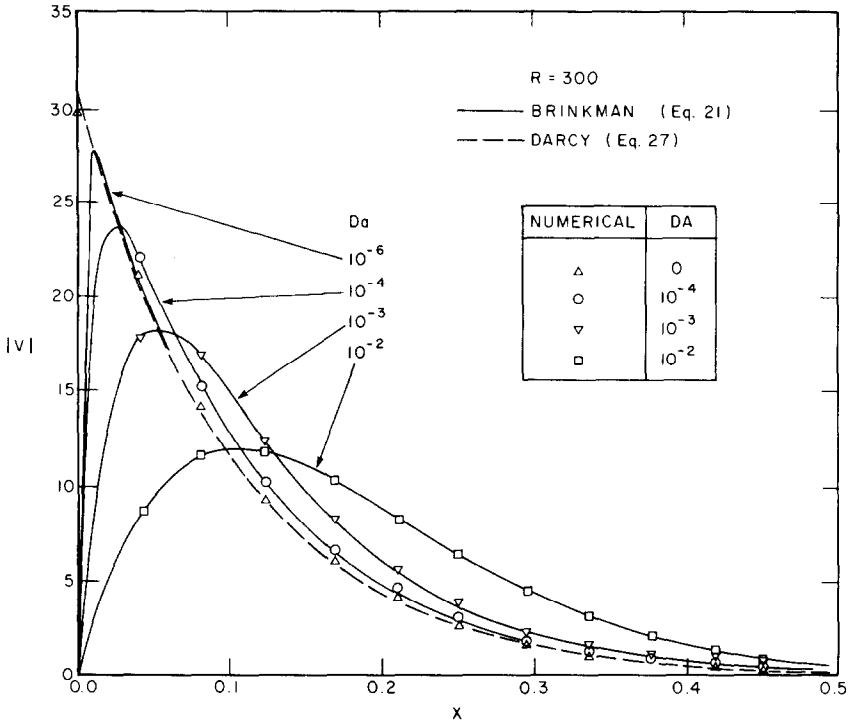

FIG. 3. The vertical velocity profile at mid-height of the enclosure as a function of Darcy number Da for $R = 300$.

velocity increases to a maximum and then drops back to zero in the core region of the enclosure. The region adjacent to the wall, where the vertical velocity increases from the zero value at the wall to the peak value, is called viscous sublayer [9]. With Darcy's model, shown as a dotted line in Fig. 3, the peak velocity is located on the wall, due to the fact that the no-slip boundary condition is not satisfied, and the thickness of the viscous sublayer is nil. As the value of Da increases the thickness of the viscous sublayer occupies gradually a larger portion of the momentum boundary layer. The position of the peak velocity x_p, i.e. the thickness of the viscous sublayer, can be obtained by solving for x in equation (21) when the velocity gradient is zero. The result is

$$x_p = \frac{4}{p\sqrt{(8/Da\,p^2 - 1)}} \tanh^{-1}\sqrt{(8/Da\,p^2 - 1)} \quad (40)$$

and as $Da \to 0$, $x_p \to 0$ asymptotically and, except in a thin region next to the wall, the velocity profile is the same as that predicted by a pure Darcy analysis. This is illustrated for the case with $Da = 10^{-6}$ in Fig. 3. As the permeability of the porous medium is increased not only does the position of the maximum velocity shift away from the wall but also its magnitude is considerably reduced. The flow is then dominated by the boundary effects and the velocity profiles approach those for a pure viscous fluid. Figure 3 shows good agreement between the numerically and theoretically predicted values of velocity profiles.

The numerical results presented in Figs. 3–7, were obtained for the case of a cavity with an aspect ratio $A = 4$. As mentioned earlier, the numerical results are independent of the aspect ratio provided that A is approximately equal to or greater than 2 [16]. The effect of Da on temperature profiles at $y = 0$ is illustrated in Fig. 4 for the case $R = 300$. All the curves have a constant slope at $x = 0$ since a constant heat flux is prescribed on the vertical walls. When Da is small enough ($Da = 10^{-6}$) the effect of the no-slip condition on temperature profiles is seen to be negligible and Darcy's model can be employed. For this situation the convective motion within the cavity is maximum since the only resistance to the flow within the porous media is due to the presence of the solid matrix. A maximum quantity of heat is extracted from the wall and its temperature drops to a minimum value. However, as the permeability of the porous media is increased, the boundary frictional resistance becomes gradually more important and adds to the bulk frictional drag induced by the solid matrix to slow down the convective motion. As a result relatively less heat is removed from the wall and its temperature increases significantly. A good agreement between the analytical solution and the numerical results is observed in Fig. 4. In fact, at the mid-height of the enclosure, the analytical and the numerical solutions were found to be in good agreement with each other provided that R is greater than approximately 20 (see Fig. 6). For lower values of R, the analytical solution, developed for the boundary layer becomes inad-

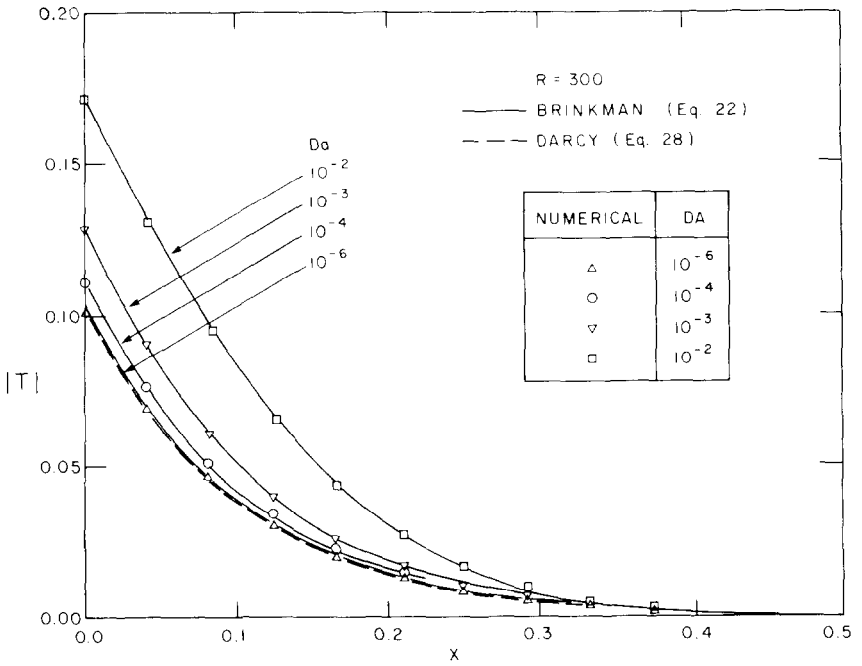

FIG. 4. The temperature profile at mid-height of the enclosure as a function of Darcy number Da for $R = 300$.

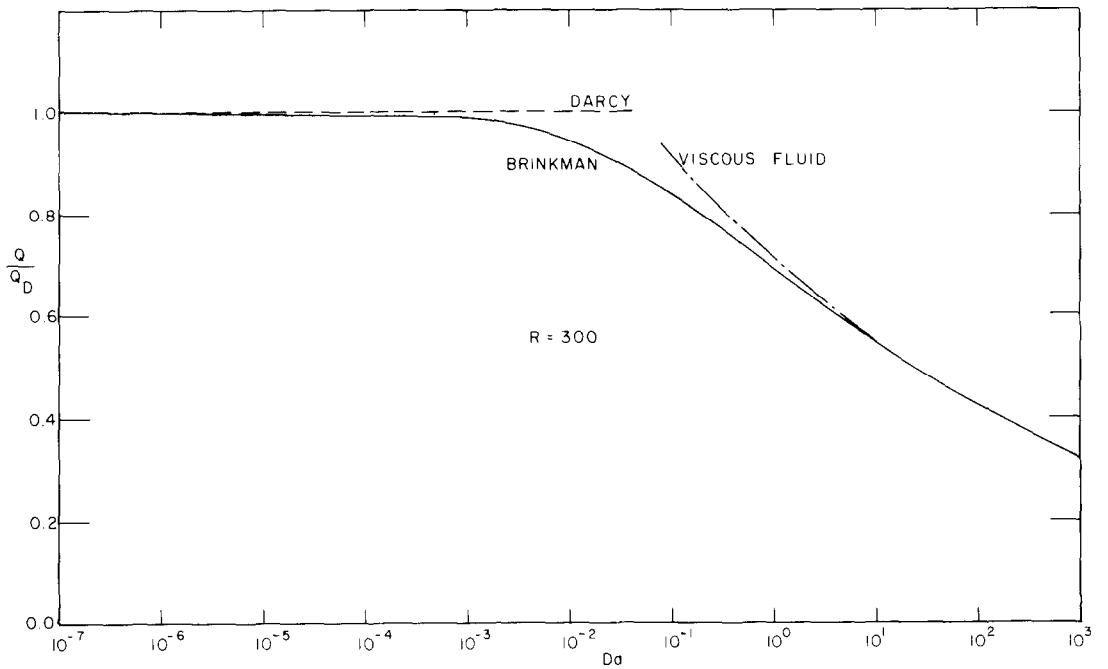

FIG. 5. Effect of Darcy number Da on the flow rate in the boundary layer at mid-height of the enclosure for $R = 300$.

equate. Also, as expected, the present solution breaks down in the vicinity of the top and bottom adiabatic walls where the fluid must flow horizontally, and the vertical temperature gradient must vanish. A similar behavior has already been reported and discussed thoroughly in the past by Bejan [12] and Kimura and Bejan [15].

The fact that the convective circulation inside the cavity is reduced as the value of Da increases is illustrated in Fig. 5 where the flow rate Q within the left boundary layer at $y = 0$ is plotted as a function of Da for the case $R = 300$. Integrating the velocity profile given by equation (21) over the thickness of the momentum boundary layer it is found that

$$Q = \frac{64R\,Da}{(Da\,p^2 - 4)^2}. \tag{41}$$

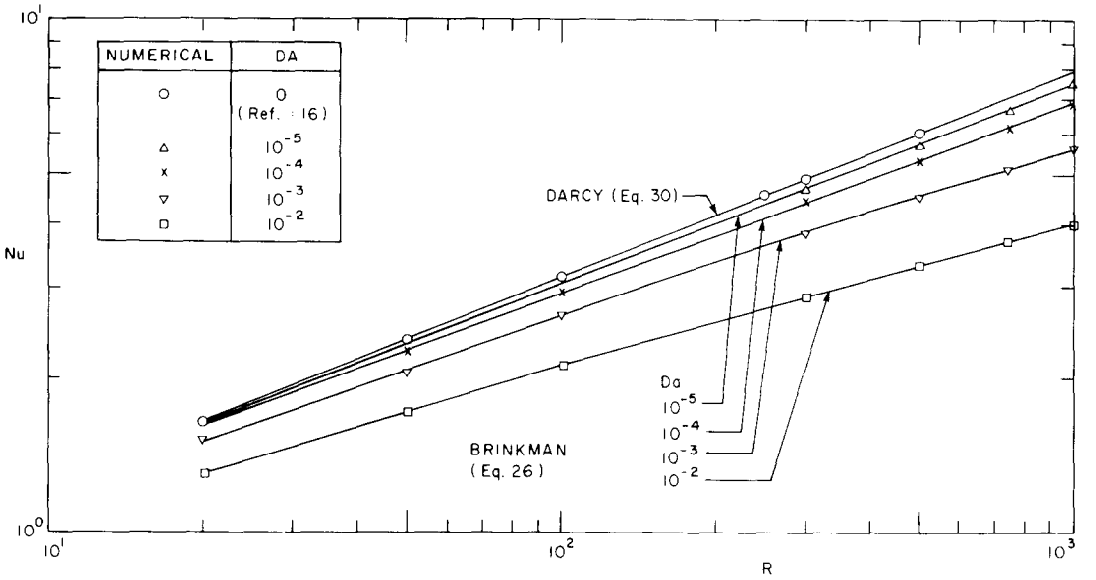

FIG. 6. Effect of Rayleigh number R and Darcy number Da on the Nusselt number Nu.

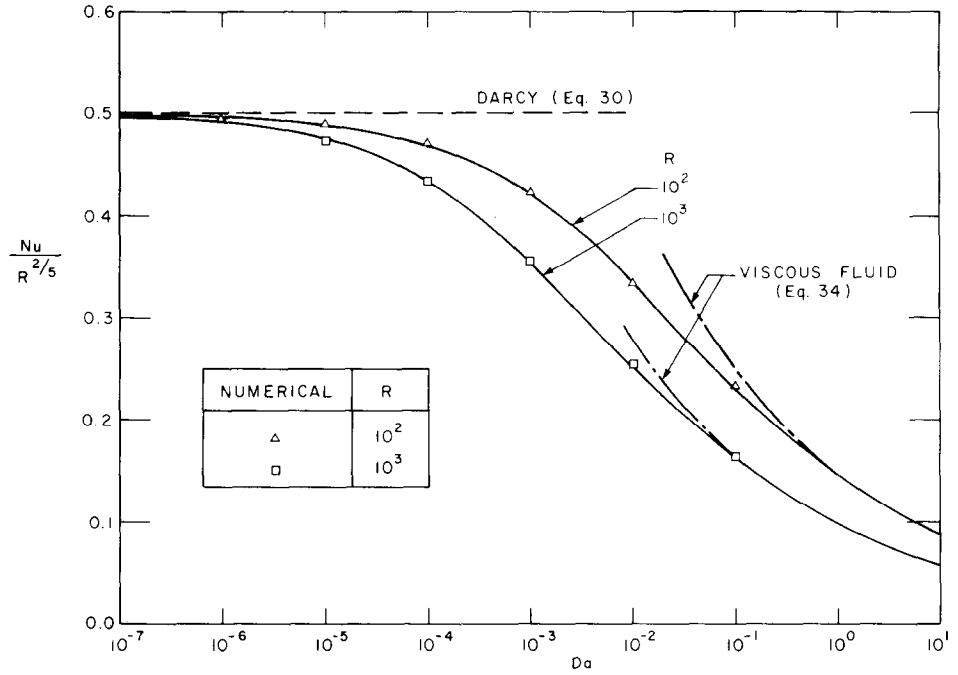

FIG. 7. Effect of Darcy number Da on Nusselt number Nu for $R = 100$ and 1000.

Similarly, integration of equations (27) and (31) yields $Q_D = R^{1/5}$ for a Darcy medium and $Q_f = 1.167Ra^{1/9}$ for a pure viscous fluid. It is seen from Fig. 5 that the flow rate predicted by Brinkman's model starts to deviate from Darcy's model when $Da \geq 10^{-4}$. As mentioned before the decreases of the flow rate result from the boundary effect, this effect increasing with the permeability of the porous medium. When $Da \geq 10$ the resistance to the flow is dominated by the boundary effect, the frictional drag induced by the solid matrix becomes relatively negligible, and the flow rate approaches that for a pure viscous fluid.

In Fig. 6 the Nusselt number given by equation (26) is plotted against the Rayleigh number for various Darcy numbers. It is seen that Bejan's solution, equation (30), based on Darcy's model is valid only for small values of Da. When $Da > 10^{-6}$ the solution of Bejan overpredicts the heat transfer across the enclosure due to the neglect of the boundary effects. This is expected since Brinkman's model provides a lower velocity, which causes less energy to be carried away from the boundary, thus causing a lower Nusselt number. For a given value of Da the deviation from Darcy's model increases as R becomes larger. Thus

for $Da = 10^{-3}$ Bejan's solution overpredicts the heat transfer by approximately 10% when $R = 20$ and 25% when $R = 1000$. Numerical solutions are presented in Fig. 6 along with the analytical solutions. It can be seen that there is an excellent agreement between the analytical solution and numerical results.

Another view of the effect of Da on the heat transfer is found in Fig. 7 where a correlation of Nu as a function of Da is presented for $R = 10^2$ and 10^3, respectively. The Nusselt number has been normalized with respect to $R^{2/5}$, i.e. half the value predicted by Darcy's law. Consequently all the curves in Fig. 7 tend towards $Nu/R^{2/5} = 0.5$ when $Da \to 0$. Results obtained from Darcy's law are valid when Da is approximately smaller than 10^{-6}. As the Darcy number is increased the value of the heat transfer within the cavity drops significantly due to the boundary effects. When Da is high enough, i.e. when the Darcy resistance due to the solid matrix becomes negligible with respect to that resulting from the boundary effects, the present solution approaches that of Kimura and Bejan [15] for a pure viscous fluid. This situation is reached when $Da \approx 1$ for $R = 10^2$ and $Da \approx 0.1$ for $R = 10^3$.

CONCLUSIONS

The effect of the no-slip boundary condition on the natural convection heat transfer in a two-dimensional porous layer with uniform heat flux from the side has been studied both theoretically and numerically. In the formulation of the problem use has been made of the viscous shear stress term due to Brinkman in order to satisfy both the no-slip and impermeable conditions on the bounding rigid surfaces. The analytical solution focuses on the boundary layer regime for which the governing equations are solved using the modified Oseen method. The boundary effects are found to slow down the buoyancy-induced flow with a resulting decrease in heat transfer. This trend is enhanced as the permeability of the porous medium increases. The present analytical solution reduces to the regular Darcy's law and viscous flow solution in the limits of low and high porosities, respectively. A good agreement is found between the analytical predictions and a numerical simulation of the same phenomenon. An improved model would also include the convective and inertial effects.

Acknowledgements—This research was supported in part by the National Research Council of Canada through grants NRC A-9201 and NRC A-4197 and jointly by the FCAC Government of Quebec, under grant CRP 507-78. The authors gratefully thank Ecole Polytechnique for providing the necessary time on an IBM 4381 computer.

REFERENCES

1. B. K. C. Chan, C. M. Ivey and J. M. Barry, Natural convection in enclosed porous media with rectangular boundaries, *J. Heat Transfer* **92,** 21–27 (1970).
2. P. Cheng, Heat transfer in geothermal systems, *Adv. Heat Transfer* **14,** 1–105 (1978).
3. Y. Katto and T. Masuako, Criterion for the onset of convective flow in a fluid in a porous medium, *Int. J. Heat Mass Transfer* **10,** 297–309 (1967).
4. K. Walker and G. M. Homsy, A note on convective instability in Boussinesq fluids and porous media, *J. Heat Transfer* **99,** 338–339 (1977).
5. T. W. Tong and E. Subramanian, A boundary-layer analysis for natural convection in vertical porous enclosures—use of the Brinkman-extended Darcy model, *Int. J. Heat Mass Transfer* **28,** 563–571 (1985).
6. S. Klarsfeld, Champs de température associes aux mouvements de convection naturelle dans un milieu poreux limité, *Revue gén. Thermique* **9,** 1403–1423 (1963).
7. G. H. Evans and O. A. Plumb, Natural convection from a vertical isothermal surface embedded in a saturated porous medium, ASME paper No. 78-HT-55 (1978).
8. K. Vafai and C. L. Tien, Boundary and inertia effects on flow and heat transfer in porous media, *Int. J. Heat Mass Transfer* **24,** 195–203 (1981).
9. J. T. Hong, C. L. Tien and M. Kaviany, Non-Darcian effects on vertical-plate natural convection in porous media with high porosities, *Int. J. Heat Mass Transfer* **28,** 2149–2157 (1985).
10. C. T. Hsu and P. Cheng, The Brinkman model for natural convection about a semi-infinite vertical flat plate in a porous medium, *Int. J. Heat Mass Transfer* **28,** 683–697 (1985).
11. J. Georgiadis and I. Catton, Free convective motion in an infinite vertical porous slot: the non-Darcian regime, ASME paper No. 85-HT-58 (1985).
12. A. Bejan, The boundary layer regime in a porous layer with uniform heat flux from the side, *Int. J. Heat Mass Transfer* **26,** 1339–1346 (1983).
13. D. Poulikakos, A departure from the Darcy model in boundary layer natural convection in a vertical porous layer with uniform heat flux from the side, *J. Heat Transfer* **107,** 716–720 (1985).
14. A. E. Gill, The boundary-layer regime for convection in a rectangular cavity, *J. Fluid Mech.* **26,** 515–536 (1966).
15. S. Kimura and A. Bejan, The boundary-layer natural convection regime in a rectangular cavity with uniform heat flux from the side, *J. Heat Transfer* **106,** 98–103 (1984).
16. P. Vasseur, M. G. Satish and L. Robillard, Natural convection in a thin inclined porous layer exposed to a constant heat flux, 8th International Heat Transfer Conference, San Francisco, Vol. 5, pp. 2665–2670 (1986).
17. G. D. Mallison and G. de Vahl Davis, The method of the false transient for the solution of coupled elliptic equations, *J. Comp. Phys.* **12,** 435 (1973).
18. P. Roache, *Computational Fluid Dynamics.* Hermosa (1976).

LE MODELE DE BRINKMAN POUR LE REGIME DE COUCHE LIMITE DANS UNE CAVITE RECTANGULAIRE AVEC UN FLUX DE CHALEUR UNIFORME SUR LES COTES

Résumé—On résume une étude analytique et numérique de la convection naturelle dans une couche poreuse rectangulaire soumise à des flux de chaleur uniformes le long des frontières verticales. Dans la formulation du problème, on utilise le modèle Darcy–Brinkman qui permet de satisfaire la condition aux limites de non-glissement. Les équations de couche limite sont résolues par une méthode modifiée de linéarisation d'Oseen. On trouve que les effets de frontière ont une influence non négligeable sur le champ d'écoulement et le transfert thermique. Ces effets sont plus prononcés dans les milieux à forte porosité pour lesquels le débit et le transfert de chaleur sont significativement réduits. Pour les faibles porosités, les résultats obtenus à partir d'un modèle avec loi pure de Darcy sont retrouvés comme un cas limite de la présente théorie. Des résultats numériques sont présentés dans le domaine $20 \leqslant R \leqslant 1000$, $10^{-7} \leqslant Da \leqslant 10$ et $2 \leqslant A \leqslant 4$. La solution analytique de couche limite s'accorde bien avec les résultats numériques.

DAS BRINKMANN-MODELL FÜR GRENZSCHICHTBEREICHE IN RECHTECKIGEN HOHLRÄUMEN BEI GLEICHFÖRMIGER, SEITLICH AUFGEBRACHTER WÄRMESTROMDICHTE

Zusammenfassung—Es werden analytische und numerische Untersuchungen der freien Konvektion in rechteckförmigen porösen Schichten, die mit einer gleichförmigen Wärmestromdichte entlang den horizontalen Begrenzungsflächen beaufschlagt werden, zusammenfassend vorgestellt. Bei der Formulierung des Problems wurde vom erweiterten Brinkmann–Modell, dem Darcy-Modell, Gebrauch gemacht, das die Haftbedingungen der Grenzschicht erfüllt. Die Grenzschichtgleichungen werden mit Hilfe einer modifizierten Oseen-Linearisierungs-Methode gelöst. Es zeigt sich, daß der Einfluß der Grenzschichteffekte auf das Strömungsfeld und den Wärmeübergang nicht zu vernachlässigen ist. Diese Effekte verstärken sich bei stark porösen Stoffen, bei denen Durchsatzrate und Wärmeübergang wesentlich kleiner sind. Bei weniger porösen Stoffen stellen die auf der Basis des Darcy-Modells gewonnenen Ergebnisse einen Grenzfall der vorgestellten Theorie dar. Numerische Ergebnisse liegen für die Bereiche $20 \leqslant R \leqslant 1000$, $10^{-7} \leqslant Da \leqslant 10$ und $2 \leqslant A \leqslant 4$ vor. Es zeigt sich, daß die analytische Grenzschichtlösung gut mit den numerischen Ergebnissen übereinstimmt.

МОДЕЛЬ БРИНКМАНА ДЛЯ ПОГРАНИЧНОГО СЛОЯ В ПРЯМОУГОЛЬНОЙ ПОЛОСТИ С БОКОВЫМ ОДНОРОДНЫМ ПОДВОДОМ ТЕПЛА

Аннотация—Приведены результаты аналитического и численного исследований естественной конвекции в прямоугольном пористом слое, нагреваемом однородными тепловыми потоками, направленными вдоль вертикальных границ. При постановке задачи применялась модель Бринкмана-Дарси, которая позволяет удовлетворять условиям нулевой скорости на границе. Уравнения пограничного слоя решались с использованием модифицированного метода линеаризации Озеена. Найдено, что граничные эффекты оказывают существенное влияние на поле течения и теплообмен. Эти эффекты больше выражены в высокопористых средах, где скорость течения и теплообмена значительно уменьшаются. Для сред с низкой пористостью данные, полученные на основе закона Дарси, рассматриваются как предельный случай предложенной теории. Численные результаты представлены в диапазонах $20 \leqslant R \leqslant 1000$, $10^{-7} \leqslant Da \leqslant 10$ и $2 \leqslant A \leqslant 4$. Показано, что аналитическое решение уравнений пограничного слоя хорошо согласуется с численными результатами.